

ULTRAVIOLET SPECTRA OF HZ HERCULIS/HERCULES X-1 FROM *HST*: HOT GAS DURING TOTAL ECLIPSE OF THE NEUTRON STAR¹

SCOTT F. ANDERSON, STEFANIE WACHTER, AND BRUCE MARGON

Astronomy Department, FM-20, University of Washington, Seattle, WA 98195;
 anderson@astro.washington.edu, wachter@astro.washington.edu, margon@astro.washington.edu

RONALD A. DOWNES

Space Telescope Science Institute, 3700 San Martin Drive, Baltimore, MD 21218;
 downes@stsci.edu

WILLIAM P. BLAIR

Department of Physics and Astronomy, Johns Hopkins University, 34th and Charles Streets, Baltimore, MD 21218;
 wpb@hut4.pha.jhu.edu

AND

JULES P. HALPERN

Columbia University, Department of Astronomy, 538 W. 120th Street, New York, NY 10027;
 jules@carmen.phys.columbia.edu

Received 1994 March 22; accepted 1994 May 23

ABSTRACT

The Faint Object Spectrograph (FOS) aboard *Hubble Space Telescope* has been used in the UV to observe the prototypical X-ray pulsar Her X-1 and its companion HZ Her. Optical spectra were also obtained contemporaneously at the KPNO 2.1 m. The FOS spectra encompass the 1150–3300 Å range near binary orbital phases 0.5 (X-ray maximum) and at 0.0 (mid-X-ray eclipse). The maximum light spectra show strong, narrow C III, N V, O V, Si IV + O IV], N IV], C IV, He II, and N IV emission lines, extending previous *IUE* results; the O III λ 3133 Bowen resonance line is also prominent, confirming that the Bowen mechanism is the source of the strong λ 4640, 4650 emission complex, also seen at maximum light. Most remarkable, however, are the minimum light spectra, where the object is too faint for reasonable observations from *IUE*. Despite the total eclipse of the X-ray-emitting neutron star, our spectra show strong emission at N V λ 1240, S IV + O IV] λ 1400, N IV] λ 1487, C IV λ 1549, and He II λ 4686 (but not the λ 4640, 4650 complex). Although this hot gas whose emission dominates the UV light at phase 0.0 might be associated with the “accretion disk corona,” it is more likely the source is somewhat less hot (but extended) gas above and around the disk, or perhaps circumstellar material such as a stellar wind.

Subject headings: stars: binaries: eclipsing — stars: individual (HZ Herculis) — ultraviolet: stars — X-rays: stars

1. INTRODUCTION

The pulsing binary X-ray source Hercules X-1 has been an intensively studied system since its discovery with *Uhuru* 20 yr ago (Tananbaum et al. 1972), and the identification of the optical counterpart, HZ Herculis, shortly thereafter (e.g., Davidsen et al. 1972). The system exhibits periodic X-ray and optical light modulation at periods of 1^s.2, 1^d.7, and 35^d, thought to represent the neutron star spin, binary orbital, and accretion disk precession periods, respectively. Because HZ Her is a late A or early F star (see § 3), the combination of the high ratio of X-ray to optical luminosity of the two stars, and their small separation, leads to a variety of prominent heating effects on the cool star during those orbital phases when its X-ray illuminated face is visible to Earth; this effect is thought to explain the 1^d.7 optical light curve, and the 1^s.2 optical pulsations, for example. Recent reviews relevant to many aspects of the Her X-1/HZ Her system (and other X-ray pulsars) may be found in White, Swank, & Holt (1983), Joss & Rappaport (1984), and Priedhorsky & Holt (1987).

HZ Her has been observed on multiple occasions with *IUE* (e.g., Dupree et al. 1978; Gursky et al. 1980). An extensive discussion and modeling of these *IUE* spectra may be found in Howarth & Wilson (1983a, b). While these *IUE* spectra cover a broad range of binary (and 35^d precessional) phases, they have (due to S/N limitations) emphasized primarily the UV spectrum outside of eclipse. This emission has usually been assumed to be some combination of that from the X-ray heated side of the A star, plus some contribution from the disk and/or mass transfer streams. In this paper, however, we report the unambiguous UV and optical detection of high-excitation, hot gas at phase 0.0, when the X-ray source is known to be eclipsed and the X-ray illuminated side of the A star is not visible.

2. UV AND OPTICAL SPECTROSCOPIC OBSERVATIONS

We obtained ultraviolet spectrophotometry of the Her X-1/HZ Her system at maximum light on 1992 April 30 (UT) and at minimum light on the 1992 May 6 (UT), using the *Hubble Space Telescope* (*HST*) Faint Object Spectrograph (FOS). These observations are part of the FOS Investigation Definition Team’s Guaranteed Time Observations program. The FOS data were obtained using the “blue detector” in the high spectral resolution mode with $\lambda/\Delta\lambda \sim 1300$, and a log of observations is given in Table 1. The large (4^o.3) FOS entrance

¹ Based on observations with the NASA/ESA *Hubble Space Telescope*, obtained at the Space Telescope Science Institute, which is operated by the Association of Universities for Research in Astronomy, Inc., under NASA contract NAS5-26555.

TABLE 1
LOG OF UV AND OPTICAL SPECTROSCOPIC OBSERVATIONS

Instrument	Wavelength Range (Å)	Exposure Time	MJD Star-End (48,000+)	1 ^{d7} Phase	35 ^d Phase
FOS G130H	1150–1600	1600s	742.572939– 742.592611	0.453–0.464	0.59
FOS G190H	1600–2350	1350s	742.699640– 742.716008	0.527–0.537	0.59
FOS G270H	2250–3300	1350s	742.633576– 742.649856	0.488–0.498	0.59
GoldCam	3500–6000	600s	754.475660– 754.482604	0.454–0.458	0.93
FOS G130H	1150–1600	1600s	748.594744– 748.614417	0.995–0.006	0.76
FOS G270H	2250–3300	1350s	748.528217– 748.544498	0.956–0.965	0.76
GoldCam	3500–6000	1800s	755.396296– 755.417130	0.995–0.008	0.95

NOTES.—1^{d7} binary orbital phases are estimated from the ephemeris of Deeter et al. (1991). 35^d precessional phases are estimated from the ephemeris of Deeter (1992), with phase zero at MJD 48477.8 and a precessional period of 34^d.9.

aperture was used (with a modest degradation of spectral resolution) to minimize the loss of light due to the pre-COSTAR spherical aberration problems. The FOS spectra have undergone the standard reductions (pair-pulsed correction, flat fielding, flux calibration, etc.) performed on all such data processed through the STScI's Routine Science Data Processing pipeline reduction software.

The maximum light FOS observations are shown in Figure 1a–1c, and encompass 1^{d7} binary phases 0.45–0.54. These maximum light observations were taken at 35^d phase 0.59. In estimating these phases, we have converted the MJD (Modified Julian Date) of the observation as supplied by STScI into a heliocentric MJED (Modified Julian Ephemeris Date), in order to more directly compare with the X-ray ephemerides of Deeter et al. (1991) and Deeter (1992); the difference between heliocentric and barycentric MJED (the latter used by Deeter et al.) is negligible for our purposes of phasing on the 1^{d7} and 35^d periods. The derivative in the 1^{d7} orbital period determined by Deeter et al. (1991) has also been accounted for in estimating the binary phases of the *HST* data. The various phases of our FOS (and optical) spectral observations, according to these Deeter et al. ephemerides, are provided in Table 1. Any remaining uncertainties in orbital ephemerides are too small to affect the conclusions of this paper. The maximum light UV FOS spectra of Figures 1a–1c confirm and extend on previous *IUE* observations and are discussed in detail in § 3.

The minimum light UV FOS spectra are shown in Figures 2a–2c; these were taken very near 1^{d7} binary phase 0.0, and 35^d precessional phase 0.76. It is crucial to note (see Table 1) that the UV spectrum of Figure 2a was taken during an interval spanning binary phases of 0.995–0.006; i.e., these data were taken very close to and even through mid-eclipse. Although *IUE* attempted multiple observations of HZ Her near X-ray eclipse, the object is too faint for that instrument when very near phase 0.0 (e.g., see spectra on microfiche in Howarth & Wilson 1983a). Thus, the minimum light FOS UV spectra (discussed in § 4) are particularly unusual, and Figures 2a–2b show a rather surprising result: high-excitation UV emission is clearly present even at mid-eclipse.

In addition to the FOS UV spectra, one of us (J. P. H.) obtained CCD optical spectra of the Her X-1/HZ Her system at both maximum and minimum light, using the GoldCam on

the KPNO 2.1 m. The instrumental setup provided coverage from 3500–6100 Å at 3.9 Å resolution. A log of these optical observations is also provided in Table 1. It should be noted that these optical observations are *not* simultaneous with the FOS UV spectra, but at least were obtained near in time to the *HST* observations. The optical spectrum at maximum is shown in Figure 1d and was obtained on 1992 May 12 (UT). The optical spectrum at minimum is shown in Figure 2d, and was obtained on 1992 May 13; this minimum light optical spectrum encompasses binary phase 0.995–0.008. The discussions in § 3 and § 4 also detail our analyses of these optical spectra at maximum and minimum light, but we again especially call attention in Figure 2d to the presence of emission, even at mid-eclipse.

3. ANALYSIS OF THE SPECTRA NEAR MAXIMUM LIGHT

The maximum light UV FOS spectra of Figures 1a–1c (also see Table 1) confirm and extend on previous *IUE* results. As found by earlier workers (e.g., Gursky et al. 1980; Howarth & Wilson 1983b), a rich emission-line spectrum in the UV is clearly evident at maximum. In our FOS spectra we detect C III λ 1176, N V λ 1240, O V λ 1371, Si IV + O IV] λ 1400, N IV] λ 1486, C IV λ 1549, He II λ 1640, N IV λ 1718, C III λ 2297, and O III λ 3133. Measurements for some of these lines are tabulated in Table 2. It is possible that C II λ 1335, A III λ 1671, and N III λ 1751 are also detected in emission; halo absorption complicates the detectability of the possible C II and A III emission, and the possible N III emission is quite broad. The range of ionization seen is not surprising, as it is likely we are observing the X-ray irradiated photosphere of HZ Her, in addition to some contribution from the accretion disk, etc. In Table 3 a list of some absorption features detected, likely due primarily to absorption from halo gas in our own Galaxy, is also provided.

The interpretation of the Ly α spectral region (see Fig. 1a) is somewhat ambiguous; most probably there is a combination of stellar line emission, stellar absorption, interstellar absorption, and perhaps some contribution from geocoronal line emission (the observations were taken with the large FOS aperture). The Ly α absorption extends over at least the range of 1211 Å to 1220 Å. If we make the simple approximation that the optical depth must be greater than or of order unity within this range, say at ± 4 Å from the line center, then the inter-

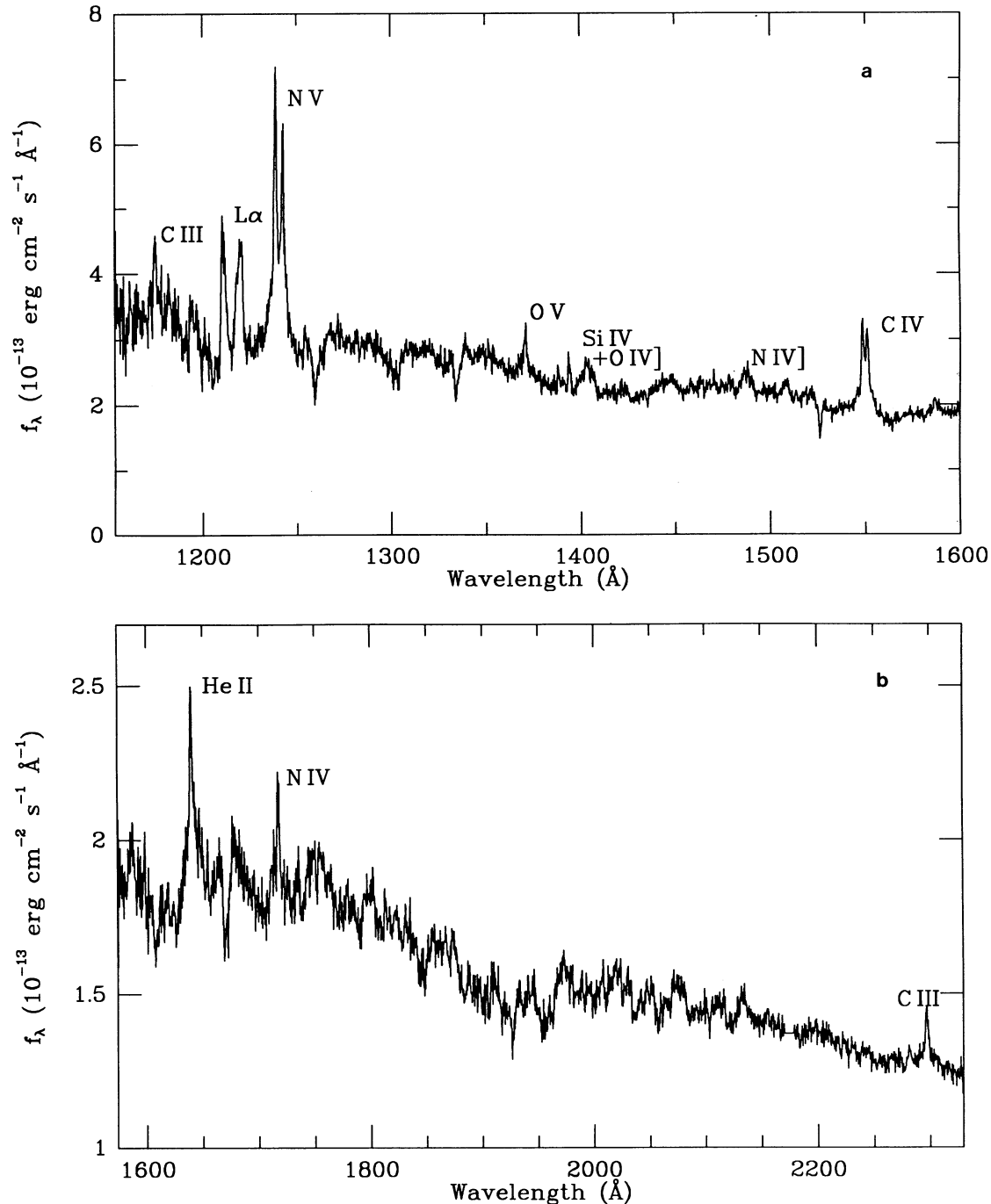


FIG. 1.—(a) The short-wavelength UV spectrum (FOS and G130H) of HZ Her near phase of maximum light. The interpretation of the Ly α region is discussed in the text. Due to the low-velocity dispersion of the emitting region, the familiar N v and C iv emission doublets are resolved, permitting good S/N estimates of the opacity of the gas at maximum light; in both cases, the ratios imply that the “MAX” gas is *not* optically thin. Note also the presence of the previously unconfirmed C iii emission line at $\lambda 1176$. The absorption lines are due to S ii, O i, Si ii, and C ii, and probably arise from interstellar galactic-halo gas. At $b = 38^\circ$, $d \sim 5$ kpc, and $m \sim 13$, HZ Her, brighter than most AGN, also serves as an excellent halo gas probe. (b) HZ Her in the mid-UV range (FOS and G190H) near maximum light. Note the presence of the high-excitation He ii $\lambda 1640$ emission, as well as a previously unreported C iii $\lambda 2297$ line. The absorptions are again likely from halo gas. The gap in the data is due to a detector cosmetic defect. (c) The near-UV spectrum (FOS and G270H) of HZ Her near maximum light. The strong Bowen O iii emission at $\lambda 3133$ is discussed in the text, and together with our measure of He ii $\lambda 1640$, provides a good S/N determination of the efficiency ($R = 0.6$) of conversion of helium photons into oxygen photons via the fluorescence process. Prominent Mg ii $\lambda 2800$ and Fe absorptions are also seen, again likely to halo gas. (d) The optical spectrum of HZ Her near maximum light. Superposed on the B star absorption spectrum are strong emission lines of C iii/N iii $\lambda\lambda 4640, 4650$ thought to be due to Bowen fluorescence, as well as He ii $\lambda 4686$ emission.

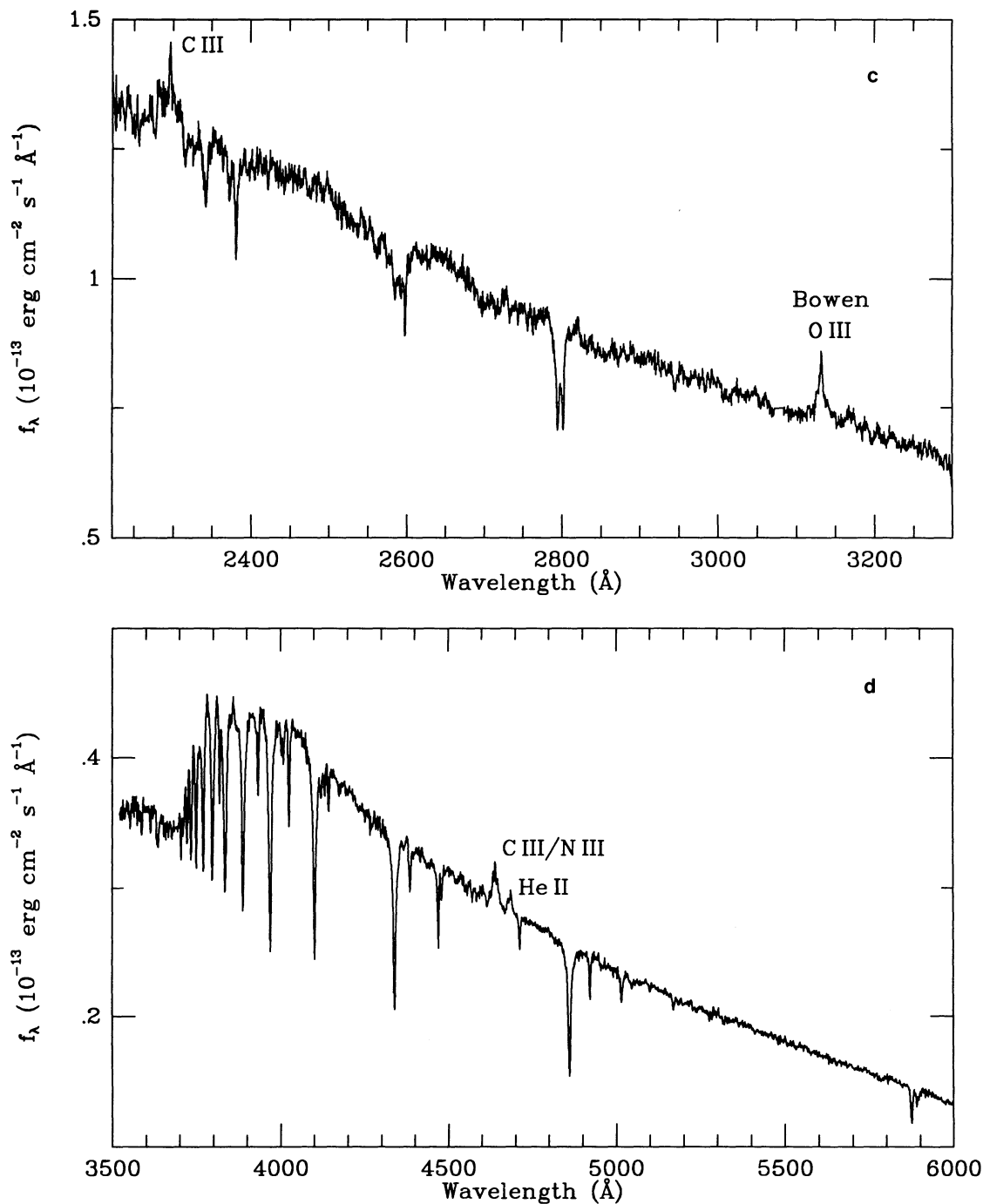


FIG. 1—Continued

vening column density of neutral hydrogen can be roughly estimated using simple relations appropriate for Ly α damping wings (e.g., Bohlin 1975). Our crude approximation here yields $N_{\text{H}} \lesssim 4 \times 10^{20} \text{ cm}^{-2}$, a value consistent with X-ray estimates (e.g., $N_{\text{H}} \sim 10^{20} \text{ cm}^{-2}$ from Vrtilik & Halpern 1985), as well as 21 cm estimates of the Galactic column density in the direction of HZ Her/Her X-1 (e.g., N_{H} of order a few times 10^{20} cm^{-2} from Heiles 1975).

The UV emission lines seen in the spectra of Figures 1a–1c provide constraints on models for the physical conditions in the gas that dominates at maximum light (e.g., see Howarth &

Wilson 1983b). For brevity, we hereafter often refer to this emission-line gas that dominates at maximum light as the “MAX” gas, although it may well arise from multiple physical sites.

The doublet ratios of both the N v $\lambda\lambda 1239, 1242$ and C iv $\lambda\lambda 1548, 1551$ lines are indicators of opacity of the MAX gas. In their analysis of *IUE* echelle spectra of the N v line, Howarth & Wilson (1983b) and Boyle et al. (1986) conclude that the N v doublet ratio is probably inconsistent with the 2:1 ratio expected of an optically thin gas. However, they also warn that the low S/N in the *IUE* echelle spectrum precludes a great deal

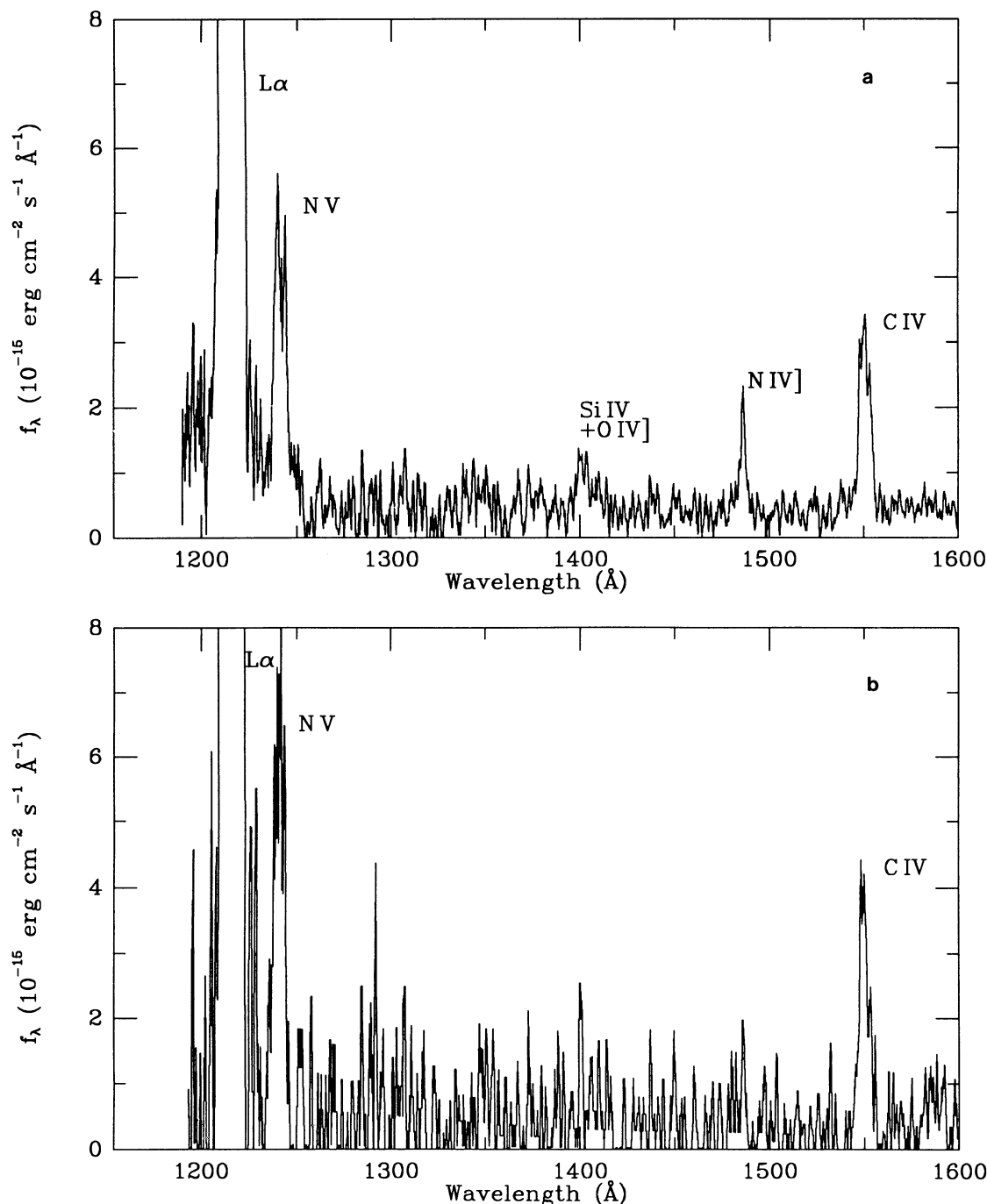


FIG. 2.—(a) The short-wavelength spectrum (FOS and G130H for 1600s) of HZ Her at mid-eclipse (binary phase 0.995–0.006). These data have been smoothed with a moving boxcar of width 5 pixels (1.3 Å). The strong Ly α emission is likely dominated by the geocorona. Despite the fact that the X-ray emitting neutron star is known to be totally occulted (and the X-ray illuminated side of HZ Her unobservable), very strong, high-excitation emission is evident. Note the clear difference in the physical conditions of the emitting “MIN” gas here from that of the “MAX” gas seen in Fig. 1a, as indicated by the greater relative strength of the collisionally de-excitable N IV], and the lack of O V in the MIN gas. (b) As in Fig. 2a, a short-wavelength spectrum (FOS and G130H) of HZ Her at mid-eclipse. Here a solitary 277s FOS readout is shown; the particular readout displayed is that which occurred nearest in time to mid-eclipse. (There are six such individual readouts summed together in the spectrum of Fig. 2a.) As in the previous figure, these data have also been smoothed with a boxcar. Each of the six separate readouts throughout the eclipse shows the unexpected presence of strong, high-excitation emission lines. (c) The solid curve shows the near-UV spectrum (FOS and G270H) of HZ Her again near mid-eclipse. Note the disappearance of the O III λ 3133 Bowen emission which was seen in the corresponding maximum light spectrum of Fig. 1c. The dotted curve shows (scaled in flux) for comparison the spectrum of HD 12311, a bright F0 V star, obtained from the IUE archive. Although the spectral resolution of the IUE data is lower, the F0 V comparison spectrum is clearly a good match to the minimum-light HZ Her spectrum. Along with the optical spectrum at minimum light (Fig. 2d), the FOS data shown here constrain the spectral type at minimum to be approximately A8–F0. Thus despite the fact that at shorter wavelengths at this same binary phase (Fig. 2a) HZ Her is dominated by high-excitation emission, here it is surprisingly normal. (d) The optical spectrum of HZ Her at mid-eclipse (binary phase 0.955–0.008). Note that the strong He absorptions present at maximum (Fig. 1d) have disappeared, as the spectral type shifts to \sim A9 during occultation of the neutron star. The $\lambda\lambda$ 4640, 4650 emission complex which was evident at maximum light (Fig. 1d) has also disappeared. The mutual disappearance of the $\lambda\lambda$ 4640, 4650 complex and the O III λ 3133 Bowen emission (Fig. 2c) lends strong support to the idea that the $\lambda\lambda$ 4640, 4650 is due to Bowen-pumped C III/N III emission. Also of particular note here is the continued presence of strong He II λ 4686 emission, even during mid-eclipse. Combined with the FOS emission spectrum of Fig. 2a, our spectroscopic data provide a direct indication of the presence of hot gas at mid-X-ray eclipse.

TABLE 2
SELECTED UV EMISSION LINES AT MAXIMUM LIGHT

Ion	$\lambda(\text{obs})$ (Å)	Flux $\times 10^{13}$ (ergs cm $^{-2}$ s $^{-1}$)	$\lambda(\text{lab})$ (Å)	FWHM (Å)	Observed Velocity (km s $^{-1}$)
C III	1175.3	2.7	1175.66	1.8	-100
N V	{ 1238.7	10.3	1238.82	2.2	-30
	{ 1242.6	8.1	1242.80	2.2	-50
O V	1371.2	1.4	1371.29	2.2	-20
Si IV	1394.0	0.5	1393.76	1.7	+35
Si IV + O IV]	1403.3	2.7	blend		
N IV	1487.6	1.4	1486.50	5.5	+220
C IV	1548.4	4.2	1548.20	2.0	+39
	1550.8	2.7	1550.77	2.4	+6
He II	1639.8	3.9	1640.34, 1640.47	4	-110
N IV	1717.8	1.7	1718.55	3.0	-130
C III	2296.6	0.8	2296.89	3.3	-40
O III	3132.0	1.2	3132.86	5.0	-80

TABLE 3
SELECTED UV ABSORPTION LINES IN MAXIMUM LIGHT SPECTRUM

Ion	$\lambda(\text{obs})$ (Å)	$\lambda(\text{lab})$ (Å)	Observed Velocity (km s $^{-1}$)
Si II	1189.5	1190.42	-230
Si II	1192.7	1193.28	-145
N I	1200	1199.90	+25
Si III	1205.8	1206.51	-175
Si II	1259.7	1260.42	-170
+S II?	...	1259.53	
O I	1301.1	1302.17	-245
Si II	1303.7	1304.37	-155
C II	1334.2	1334.53	-75
Si II	1526.2	1526.72	-100
Al II	1669.5, 1672.4	1670.81	
Fe II	2341.4	2344.21	-360
Fe II	2372.4	2374.46	-260
Fe II	2380.7	2382.76	-260
Fe II	2585	2586.64	-190
Mn II	2592.1	2594.50	-275
Fe II	2597.8	2600.18	-275
Mg II	{ 2794.6	2796.35	-190
	{ 2801.3	2803.53	-240

of confidence in this assertion. The higher S/N and good spectral resolution of our FOS spectra allow a more accurate determination of the N v doublet ratio at maximum. In addition, our *HST* spectra provide the C iv doublet ratio as well; the C iv doublet has not been resolved in any previous spectra. In order to deblend and fit (via χ^2 minimization) these doublets, we used the IRAF task called "specfit" (Kriss 1994); this task also yields error estimates for the profile fits/deblends. Because of the pre-COSTAR spherical aberration problems, the line profiles in spectra taken through the 4"3 FOS aperture are distinctly non-Gaussian, and have rather broad wings. Modeling the doublet components as single Gaussians was therefore found to be inadequate, but an ensemble of Gaussians (to approximate both the line profile "cores" and "wings") provided good fits. From our FOS data, and this line fitting/deblending approach, we estimate doublet ratios of 1.3 ± 0.1 and 1.6 ± 0.2 at maximum light for, respectively, N v and C iv, thus implying that the MAX gas is *not* entirely optically thin in either line. Although of lower S/N, recent Hopkins Ultraviolet Telescope data (Blair et al. 1994) which resolve the O vi $\lambda\lambda 1032, 1038$ doublet at maximum light in HZ Her/Her X-1

are also consistent with such doublet ratios. (It should be noted that there is an additional small systematic uncertainty in the intrinsic line strengths and ratios for some emission lines—e.g., C iv—that arises due to possible absorption in the intervening galactic halo gas.)

Howarth & Wilson (1983b) undertook a careful analysis of (especially) the line ratios of nitrogen and carbon to estimate the physical conditions in the MAX gas. They infer a temperature of about $T \sim 32,000$ K and a density of $n_e \sim 2.0 \times 10^{13}$ cm $^{-3}$. As we find at least rough agreement between *IUE*- and *FOS*-determined values for most of these line ratios, a similar analysis of the *HST* spectra would be expected to yield very similar results. However, Howarth & Wilson (1983b) also concluded that the gas physical parameters they derived might be incompatible with the presence of strong C III $\lambda 1176$ and C III $\lambda 2297$; their *IUE* data apparently lacked sufficient S/N to conclusively reveal or exclude these lines. Our *FOS* data (Figs. 1a, 1c) show that both these permitted C III lines are present at maximum light, suggesting that some modifications of their earlier conclusions for the physical conditions in the MAX gas may be required.

In general, the velocity centroids of the emission lines might also offer clues to the location of the line emitting region(s) for the MAX gas. Previous studies (e.g., Boyle et al. 1986) have utilized high-resolution *IUE* observations of the N v doublet and indicate that the velocities of the MAX gas emission are consistent with an origin in the X-ray heated atmosphere of HZ Her. The 1 d 7 orbital phasing of our observations (here at phase 0.5) does not permit a very sensitive velocity test for the MAX gas, as the binary companions are moving transverse to the line of sight. Most of the UV emission lines at maximum light have velocity centroids more-or-less consistent with the systemic velocity of about -60 km s $^{-1}$ (e.g., Crampton & Hutchings 1974); all the strong UV emission lines at maximum light have velocities in our data that are within ~ 100 km s $^{-1}$ of this value. These line velocities are listed in Table 1, but note that values quoted there are observed velocities, and do not have the small (~ 10 km s $^{-1}$) heliocentric and spacecraft corrections applied. Some caution may be prudent in interpreting these velocities and their apparent dispersion. When special wavelength calibration exposures are not obtained at the same time as the science observations (this is the usual situation, and is the case for these *FOS* data), the uncertainty in radial velocities is expected to be ~ 60 km s $^{-1}$ (see chap. 16 in Baum 1994, or Kriss, Blair, & Davidsen 1992). Thus, we feel it would cur-

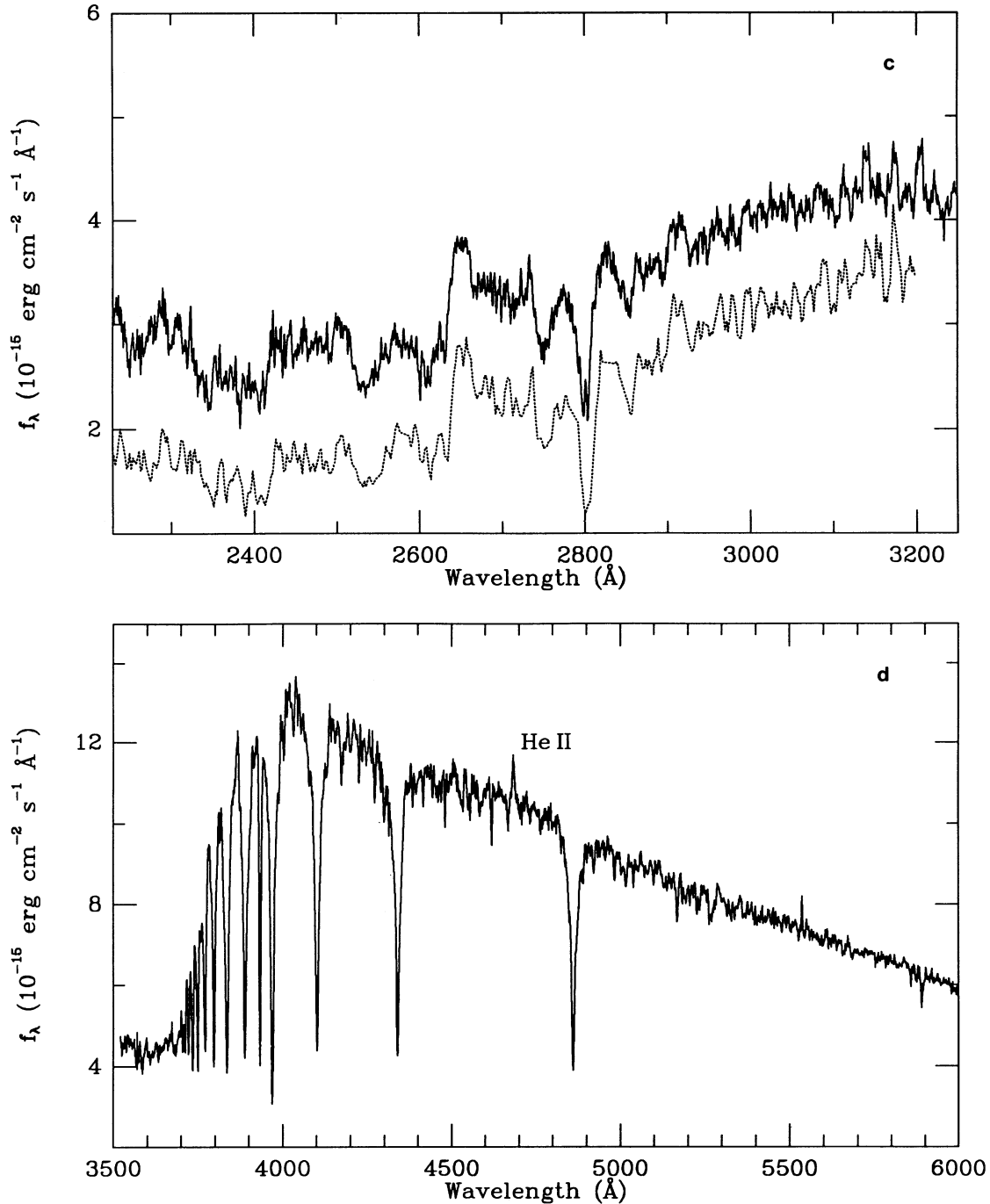


FIG. 2—Continued

rently be premature to attribute the dispersion in velocities seen in Table 1 to a physical rather than instrumental cause.

The velocity widths of the *cores* of the UV emission lines in the MAX gas are, in general, consistent with their being unresolved at the instrumental resolution of $\sim 220 \text{ km s}^{-1}$. However, the velocity width information from these data must again be interpreted conservatively. As noted above, the poor pre-COSTAR FOS line spread function is particularly unusual in shape (e.g., with very broad wings) for the 4"3 hole used for these observations. In these data, the majority of the emission-line flux is observed to fall in these broad wings rather than in

the unresolved cores. Therefore, although the broad wings observed here are quite plausibly (and even likely) an instrumental effect, our data do not convincingly preclude the possibility that the majority of the emission-line flux arises in material having typical Keplerian and/or escape velocities in the system. Such velocity issues may be better empirically determined via post-COSTAR observations of the Her X-1/HZ Her system, using the FOS and a smaller aperture.

The contemporaneous optical spectrum at maximum light is shown in Figure 1d. As has been reported by many earlier workers (e.g., Crampton & Hutchings 1974), the maximum

light optical spectrum displays strong He II $\lambda 4686$ and the C III/N III $\lambda\lambda 4640, 4650$ complex. Except for the emission lines, the optical light spectrum at maximum of Figure 1d is similar to that of a B star (perhaps \sim B3–B6). However, it is not a sufficiently good match to any normal MK standard star spectrum to permit a precise classification; for example, the strength of the Balmer jump is anomalously low compared to that expected for a normal B star. This lack of a precise match to a normal star is hardly surprising, given that much of the light here is probably associated with the X-ray heated atmosphere of HZ Her (itself having an extended atmosphere), plus some contribution from the accretion disk, etc. Note also that the X-ray heating effects are expected to change as a function of 35^d phase as the accretion disk precesses, and the X-ray shadow it casts causes a change in the X-ray illuminated area on HZ Her (e.g., Gerend & Boynton 1976).

Along with many other X-ray binaries, HZ Her shows the blend of C III/N III $\lambda\lambda 4640, 4650$ emission lines at far greater strength than expected for reasonable abundances: note the strength of this complex in the maximum light optical spectrum of Figure 1d. McClintock et al. (1975) proposed that this feature is due to Bowen fluorescence, a pumping mechanism also seen in gaseous nebula and AGN (see Schachter, Filippenko, & Kahn 1989 and Liu & Danziger 1993 for recent reviews), resulting from the near coincidence of He II Ly α $\lambda 304$ with an O III $\lambda 304$ line. Support for this hypothesis in the specific case of HZ Her was provided by the detection of an additional predicted Bowen line, O III $\lambda 3444$, in HZ Her by Margon & Cohen (1978). However, the strongest predicted Bowen line (4 times the strength of $\lambda 3444$) is O III $\lambda 3133$, which is very awkward to observe from the ground. Note the prominence of this feature in our *HST* spectrum of Figure 1c. Our measures of He II $\lambda 1640$ and O III $\lambda 3133$ emission lines in the FOS UV spectra provide a high S/N determination of the efficiency, R , with which the He II Ly α photons (assumed to be produced by recombination) are converted via Bowen fluorescence into O III photons in the MAX gas. The earlier, but highly uncertain, *IUE* measure of Howarth & Wilson (1983b) yielded a value of $R = 2$. Our data yield a value of $R = 0.6$ (assuming case B), comfortably below the recombination limit of $R = 1$ (and similar to the value Schachter et al. 1989 find for Sco X-1).

4. ANALYSIS OF THE SPECTRA AT MID-ECLIPSE

The shortest wavelength UV FOS spectrum (FOS G130H; Fig. 2a) at mid-eclipse of the X-ray source shows an obvious and very surprising result. The system inclination is known to be close to 90°, and so the neutron star is totally eclipsed, and the X-ray illuminated side of HZ Her is unobservable; yet strong, high-excitation emission lines of N V, Si IV + O IV], N IV], and C IV are clearly evident even at binary phase 0.995–

0.006! (The situation at Ly α is confused, particularly due to possible geocoronal contamination in the large aperture.) We also note that the FOS data were read out every ~ 5 minutes during the 1600 s total exposure shown in Figure 2a. At least the C IV and N V emission lines are detected in *each* of the individual readouts during the passage through mid-eclipse; for example, Figure 2b shows that solitary 5 minute readout closest to mid-eclipse. Table 4 provides information on some of the UV emission lines seen at minimum light.

The physical conditions in the gas that dominates the UV emission at minimum light (hereafter, often called the “MIN” gas) are obviously rather different than those in the MAX gas. For example, compare the relative strengths of N IV] $\lambda 1487$ and O V $\lambda 1371$ between the two binary phases (compare Figs. 2a and 1a). The greater relative strength of (the collisionally de-excitable) N IV] in the MIN gas, and the apparent absence of O V $\lambda 1371$, are probably indicative of a lower density and temperature than for the MAX gas. More quantitative inferences on the MIN gas physical conditions are provided at the end of this section, but here we note that the critical electron density for collisional de-excitation of N IV] is a few times 10^{11} cm⁻³.

The near UV spectrum (G190H) near mid-eclipse is shown in Figure 2c, as the upper solid line. The *lack* of emission present at this phase in the near-UV is noteworthy: in particular, note the absence of the O III $\lambda 3133$ Bowen line near mid-eclipse (and compare to Fig. 1c). Indeed the near-UV spectrum of HZ Her in Figure 2c is a good match (in this wavelength range) to that of a normal late A or early F star; for comparison, the lower and dotted curve in Figure 2c displays a (scaled) *IUE* spectrum of the bright F0 V star HD 12311.

The contemporaneous optical spectrum at minimum light is shown in Figure 2d, and encompasses binary phase 0.995–0.008. As has been known for many years, when the X-ray source is eclipsed, the optical spectrum changes from B to late A or early F. Combined with our near-UV spectrum of Figure 2c, our optical spectrum of Figure 2d allows us to constrain the spectral type of HZ Her to about A8–F0, by comparison with stars in the Jacoby, Hunter, & Christian (1984) library of stellar spectra. However, because of the modest spectral resolution of the optical data, and the modest S/N of the UV data at minimum light, we are unable to conclusively determine a luminosity class for HZ Her at minimum from these data.

Note also from the optical spectrum at minimum (Fig. 2d) that the C III/N III $\lambda\lambda 4640, 4650$ complex has disappeared near mid-eclipse. As noted above, the Bowen O III $\lambda 3133$ is also absent (or very weak) at minimum light (Fig. 2c), and this mutual disappearance strongly suggests that the Bowen mechanism is indeed responsible for the $\lambda\lambda 4640, 4650$ complex. (It should be kept in mind, however, that the optical and UV spectra are only contemporaneous, and not simultaneous.)

TABLE 4
UV EMISSION LINES AT MINIMUM LIGHT

Ion	λ (obs) (Å)	Flux $\times 10^{14}$ (ergs cm ⁻² s ⁻¹)	λ (lab) (Å)	FWHM (Å)	Observed Velocity (km s ⁻¹)
N v	1239.5	1.5	1238.82	3.5	+165
	1243.7	1.2	1242.80	2.6	+217
Si iv + O iv]	1400.4	0.5	Blend		
N iv	1486.4	0.6	1486.50	3.3	-20
C iv	1548.9	1.0	1548.20	4.0	+136
	1552.2	0.8	1550.77	3.3	+277

Evidently, most of the Bowen emission arises from either the disk and/or the X-ray illuminated side of the A star, or another site that is fully eclipsed at phase 0.0.

Finally, note in the minimum light optical spectrum of Figure 2*d* that He II $\lambda 4686$ emission (excitation potential, 51 eV) is still present at mid-eclipse. A previous report of this phenomenon has been made by Koo & Kron (1977). Thus, both the FOS (Fig. 2*a*) and optical spectra (Fig. 2*d*) at minimum light confirm the presence of another site of hot gas in the system. This site is either noncoincident and/or more extended than the traditionally discussed locales of the disk and X-ray illuminated side of the A star. Moreover, the site responsible for the MIN gas is evidently distinct from that producing the Bowen-related MAX gas emission.

Regardless of the location of the MIN gas, the FOS UV data of Figure 2*a* are useful in constraining models of the physical conditions of the gas. As a first look at this issue, we have used the XSTAR software written by Kallman & Krolik (1993). This software calculates physical conditions and model emission spectra of photoionized gases, for a given input ionizing spectrum, ionization, parameter, N_p (column density of hydrogen, neutrals plus ions), and elemental abundances, plus initial guesses at the gas density and temperature.

For optimal use of such model calculations, it is important to account for the opacity of the ionized gas. At minimum light, the spectra of Figure 2*a* have inadequate S/N to provide definitive doublet ratios for N v and C iv; however, our best estimates are $\sim 1.3 \pm 0.4$ for both N v and C iv. On the one hand these values are consistent at the 1σ level with the doublet ratios for the MAX gas, but on the other hand, they are also consistent at the 2σ level with the ratio $\sim 2:1$ expected for the optically thin case. We hence make the further simplifying assumption (perhaps wrong in detail) that the MIN gas is optically thin.

In these initial XSTAR models, we also make several additional simplifying assumptions. We assume normal solar abundances (although it would not be surprising to find nonsolar abundances in an interacting neutron-star binary system). As a representative input ionizing X-ray spectrum, we use the simple description of the high-state X-ray spectrum discussed in Vrtilik & Halpern (1985); this includes both a soft X-ray blackbody component, and a power-law component at higher energies. (It may be recalled that Her X-1 has a strong soft X-ray component—e.g., McCray et al. 1982—which is not adequately described as a simple continuation of the higher energy, approximately power-law X-ray spectrum.) We consider a range of normalizations (in the 0.1–20 keV band) from $L_x \sim 2 \times 10^{35}$ ergs s^{-1} to $L_x \sim 2 \times 10^{37}$ ergs s^{-1} . The smaller value of L_x is a reasonable lower limit, even for material quite near the disk rim which might not always have an unobscured view to the central X-ray source; this value is similar to the luminosity inferred, for an assumed distance of 5.8 kpc (Oke 1976), from the residual X-ray flux present at mid-eclipse (see § 5). The larger value of L_x is a reasonable upper limit, consistent with the inferred high-state X-ray luminosity. We assume that the MIN gas arises in a spherical shell of constant density at a distance of at least $r > 3 \times 10^{11}$ cm from the neutron star (extending beyond the limb of the A star even at mid-eclipse).

With these assumptions, we explore some possible model physical conditions of the MIN gas that are approximately compatible with the observed UV emission-line spectrum of Figure 2*a*. Here, we look for an overall agreement or contradiction between the model spectrum and the observations. In

particular, we consider the model to be in approximate “agreement” with the observations if the model predicts that the four strongest lines (longward of Ly α and shortward of 1640 Å) are the same as the four strongest lines observed in the FOS spectrum of Figure 2*a*, namely N v, Si iv + O iv], N iv], and C iv. We do not attempt to precisely match the specific line ratios among even these four lines. For example, we are unable—with the above assumptions—to identify models which yield a N v/C iv ratio exceeding unity; the observed value in the MIN gas is N v/C iv ~ 1.5 . Such a large N v/C iv ratio is contrary to many theoretical calculations (e.g., Hatchett, Buff, & McCray 1976) for an optically thin, X-ray heated gas of solar abundance, but is also observed in other low-mass X-ray binaries (e.g., Cordova & Howarth 1987). More sophisticated modeling of the geometry and of the multiple ionizing sources (e.g., disk, reheated surface of the A star, accretion disk corona, direct pulsar X-ray emission, etc.), and a relaxation of the assumption of solar abundances might be expected to produce a better match between model and observed UV spectra.

Keeping in mind our simplifications, an overall “agreement” (in the sense described above) is obtained from XSTAR models if the extended MIN gas has a density of $n_e \lesssim 10^{11}$ cm^{-3} , a temperature of 15,000 K \lesssim 33,000 K, an ionization parameter of $10^0 \lesssim \xi \lesssim 10^1$ (where ξ is in units of ergs cm s^{-1}), and a hydrogen column density (ions plus neutrals) of $N_p \gtrsim 10^{19}$ cm^{-2} . Above a density of $n_e \gtrsim 10^{11}$ cm^{-3} , the N iv] emission in the XSTAR model spectra is strongly suppressed, due to collisional de-excitation. For higher ionization parameters (and hotter gas), the XSTAR models predict the presence of strong O v $\lambda 1371$ emission, in contradiction to the observed spectrum at minimum light; for lower ionization parameters (and cooler gas), the XSTAR models predict the presence of strong C II $\lambda 1335$ line emission (or other low-ionization species), but strong C II is not evident in the FOS spectra of the MIN gas.

The C iv and N v emission lines of the MIN gas have inferred luminosities of order $L \sim 10^{32}$ ergs s^{-1} , for the adopted distance of 5.8 kpc. For values of N_p below $\sim 10^{19}$ cm^{-2} , the XSTAR models yield insufficient luminosities in these UV emission lines, even when the input ionizing spectrum has the higher normalization of $L_x \sim 2 \times 10^{37}$ ergs s^{-1} . For the alternate minimum normalization of $L_x \sim 2 \times 10^{35}$ ergs s^{-1} , values of $N_p \gtrsim 10^{21}$ cm^{-2} are needed in order to yield adequate luminosities in the UV emission lines. Such estimates of N_p are really lower limits because the covering factor of the MIN gas is uncertain, and here $\Omega/4\pi = 1$ was assumed; the fraction of the MIN gas that is actually hidden from observation at mid-eclipse is also uncertain. Finally, if we further invoke a plausible, but not definitive, restriction that the MIN gas is located within the characteristic dimensions of the binary orbit, $a \lesssim 10^{12}$ cm, then we also have $N_p \sim a \times n_e$, and hence $N_p \lesssim 10^{23}$ cm^{-2} .

5. DISCUSSION

Despite the surprising presence of the emission evident in Figures 2*a* and 2*d*, there have actually been bits and pieces of evidence for many years indicating that hot gas is visible from HZ Her even during mid-eclipse. For example, in a little-cited observation almost two decades ago, Koo & Kron (1977) reported an incident of He II $\lambda 4686$ in emission at mid-eclipse on a glass plate obtained in 1973 in a heroic 6 hr (purposely trailed) exposure by R. Kraft. Given our results of Figure 2*a*

and 2*d*, it now seems possible that this is a common or perhaps even ubiquitous feature of the system at minimum. The detection of He II $\lambda 4686$ emission at mid-eclipse is not unique to Her X-1, but it may be more surprising in this system. The unusual X-ray binary 2A 1822–371 has also been shown by Mason et al. (1982) to exhibit $\lambda 4686$ emission during X-ray mid-eclipse, and this is thought to arise from an “accretion disk corona” (ADC). At least the high-excitation $\lambda 4686$ emission (but not necessarily the lower excitation UV emission lines) in the HZ Her/Her X-1 MIN gas might also arise in an ADC. However, in the case of 2A 1822–371, the compact object is thought to be more massive than the companion, and hence the disk and/or ADC is less likely to be fully occulted by the companion star at mid-eclipse than in the HZ Her/Her X-1 system.

There are now several X-ray studies suggesting the presence of extended hot gas in Her X-1, perhaps from multiple sites. For example, Mihara et al. (1991) provide X-ray spectral evidence for an ADC from their low-state *Ginga* observations. The upper limit ($r \leq 5 \times 10^{11}$ cm) they estimate for the size of their “soft component”—the component they identify with the ADC—is marginally large enough for visibility at mid-eclipse; for this ADC, they estimate an ionization parameter of $\xi \geq 10^3$ and a density of $n_e \geq 8 \times 10^{10}$ cm $^{-3}$. On the other hand, Mihara et al. also provide X-ray spectral evidence for the presence of a more extended X-ray scattering region, which they term the “hard component.” They estimate the following basic parameters for this more extended gas: $\xi \leq 10^2$, $n_e \leq 5 \times 10^{12}$ cm $^{-3}$, $N_H \approx 10^{24}$ cm $^{-2}$, and located at a minimum distance of $r \gtrsim 2 \times 10^{11}$ cm from the neutron star. Although a range of gas physical parameters are allowed, Mihara et al. prefer to attribute their “hard component” to material near the outermost rim of the accretion disk.

There are now also several reports of the detection of nonzero X-ray emission at mid-eclipse. Such detections have been reported from *EXOSAT* (Parmar et al. 1985), *ROSAT* (Mavromatakis 1993), and *Ginga* (Choi et al. 1994a). Choi et al. and Parmar et al. argue for the presence of an extended wind, perhaps excited by X-ray illumination of the A star and/or outer regions of the disk. (The notion of a wind in Her X-1 extends back at least as far back as Arons 1973 and Davidson & Ostriker 1973; see also, for example, McCray & Hatchett 1975 and Begelman & McKee 1983). A very extended wind as suggested by such X-ray observations could, in a geometrical sense, clearly manifest itself in UV emission at mid-eclipse (although there is little evidence in the maximum light UV spectra for common signatures—P Cygni profiles, etc.—of a wind).

However, in addition to a very extended region such as a wind, we must also consider an alternate geometric possibility that the emission seen in Figure 2*a* arises merely from the edge of a standard accretion disk, peeking out beyond the limb of the A star at mid-eclipse. To test this idea, we have computed the consequence of several simple geometrical models of the system, using details and parameters (orbital inclination, disk tilt, disk flare angle at outer rim, disk radius, “radius” of the A-star, binary separation, and phase offset between disk line of nodes and 35^d X-ray phase zero-point) described in and derived from earlier optical studies of the Her X-1 system (Gerend & Boynton 1976; Howarth & Wilson 1983a; Boyle & Howarth 1988). For all three of these models, the geometry is such that a simple cylindrical disk (e.g., one not twisted) is totally eclipsed by the A star at phase 0.00 and 35^d phase 0.76 (see Fig. 3). Thus, the emission seen in the FOS spectrum of

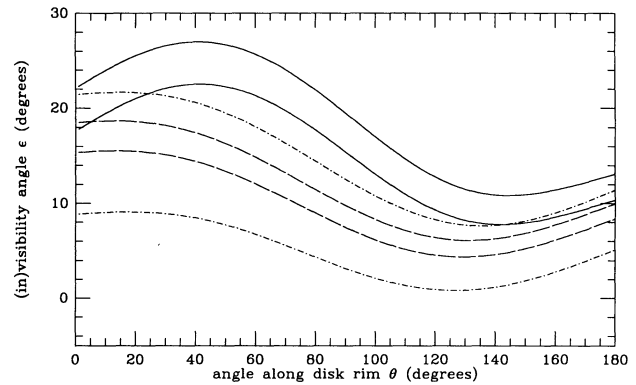


FIG. 3.—The geometrical visibility of a simple cylindrical disk beyond the limb of the occulting A star at binary phase 0.00 (mid-eclipse) and 35^d phase 0.76 (i.e., the same 1st and 35^d phases as the FOS spectra of Figs. 2*a*–*b*). The ordinate shows the angle ϵ , for an observer at the rim of the accretion disk, between the direction to Earth and that to the limb of the A star. For angles $\epsilon > 0^\circ$, the limb of the A star occults the line-of-sight view to Earth, and in turn an Earth-based observer cannot see the disk rim. The angle ϵ is plotted as a function of θ , the angle along the disk rim relative to the disk line of nodes (intersection of the disk mid-plane and the binary orbit). For simplicity, only the 180° range of θ potentially having the greatest visibility is plotted. The geometrical visibilities for three sets of simple disk parameters, derived from optical/UV studies, are depicted: the solid lines depict the disk parameters estimated by Boyle & Howarth (1988), the dashed lines are for those estimated by Howarth & Wilson (1983a), and the dot/short-dashed lines are for those estimated by Gerend & Boynton (1976). For each set of parameters, there are two lines plotted which depict the range in the “disk flare” angle or disk thickness parameter (see text and the individual references). None of the three pairs of curves attain values of $\epsilon < 0^\circ$, and visibility is nearly attained only for the Gerend & Boynton parameters. We conclude that with currently believed parameters, a simple disk about the neutron star is expected to be completely occulted by the A star at the 1st and 35^d phases corresponding to our detection of the (evidently extended) UV emission seen in Figs. 2*a*–*b*. It is thus unlikely that the observed minimum light UV emission comes from the region typically ascribed to the disk.

Figure 2*a* at minimum appears to arise from a region distinct from that typically associated with a simple accretion disk. (Note that the optical $\lambda 4686$ emission of Fig. 2*d* could come from the outer edges of a disk, using even traditional system parameters; these optical data were taken at a less stringent 35^d precessional phase for such a test.)

On the other hand, in closing these geometrical arguments, it should be noted that it is *not* possible to exclude all conceivable disks, or related material near the disk rim, as the site for the UV emission of the MIN gas evident at mid-eclipse. This residual uncertainty arises because the A star eclipses the *entire* Roche lobe of the neutron star only for orbital inclinations of $\gtrsim 85^\circ$. The aforementioned, optical/UV-constrained models include values as low as 81° (Gerend & Boynton 1976) for this angle. Thus, while it is unlikely that the MIN gas arises from a simple disk having “standard” parameters, we are not able to rule out completely (for example) an origin for the MIN gas emission at the rim of a more highly tilted, thicker, or unusually twisted accretion disk, that more nearly fills the Roche lobe of the neutron star. UV/optical observations of emission at mid-eclipse at different 35^d phases than those sampled here might help resolve this issue.

In addition to an ADC, a possible extended wind, or just the outer regions of an unexpectedly large (or thick, or tilted, or twisted) accretion disk, at least one other additional warm component of gas has been inferred to be associated with the Her X-1 system. Erratic “X-ray dips” have been attributed to absorbing material in the line of sight (e.g., Giacconi et al.

1973; Crosa & Boynton 1980; Boynton, Crosa, & Deeter 1980; Vrtilik & Halpern 1985; Voges et al. 1985; Choi et al. 1994b). These blobs are also indirectly inferred in some previous UV and optical studies (e.g., Howarth & Wilson 1983b; Bochkarev & Karitskaya 1989 and references therein), and may be related to the mass transfer process from the A star to the disk around the neutron star. In some models, the blobs of material are thought to occupy a very extended region above and around the accretion disk; for example, Bochkarev & Karitskaya (1989) propose a model in which such relatively cool (but still $T \sim 30,000$ K) blobs might be in pressure equilibrium with the much hotter ADC, and be visible even during mid-eclipse. Bochkarev & Karitskaya (1989) estimate that the blob mass may be transferred above the plane of the disk up to a height of ~ 0.6 times the disk radius. The simple geometrical model discussed above confirms that such high material should be visible peeking out beyond the limb of the A star even at mid-eclipse (for the 35° phases observed here). Thus such blobs might also be responsible for the emission we observe at mid-eclipse in Figures 2a and 2d.

Finally, we note that although our measurements are not very reliable (due to the low S/N), the velocity centroids of the UV lines at mid-eclipse (Table 4) indicate that the MIN gas could be redshifted by up to a few hundred km s^{-1} with respect to the line velocities observed at binary phase 0.5. Such velocities for the MIN gas are similar in magnitude to those expected for Keplerian or escape velocities from the system, and a redshift could be consistent with an anisotropic wind emanating from the X-ray illuminated side of the A star or the disk. Such redshifted velocities, if confirmed, might also be inconsistent with expectations for the most geometrically visible portion of an extended outer disk region, assuming Keplerian orbits in a counterprecessing simple (e.g., untwisted) disk system. Again, further UV and optical observations of the MIN gas, taken at additional 35° phases to those discussed here, might allow a more definitive resolution of this velocity issue.

6. SUMMARY

We have obtained *HST*/FOS UV spectra and contemporaneous ground-based optical spectra of the prototypical binary X-ray pulsar system Her X-1/HZ Her; spectra were taken near phase 0.5 (X-ray maximum on the binary period), and at binary phase 0.0 (X-ray mid-eclipse). The UV and optical spectra at minimum light were taken very close to, and even pass through, mid-eclipse.

The maximum light spectra show strong, narrow C III, N V, O V, Si IV + O IV], N IV], C IV, He II, N IV, and O III emission lines. The high S/N and resolution of the FOS UV spectra at maximum provide good indicators of the opacity of the "MAX" gas, from the doublet ratios of both the N V and C IV lines. We estimate ratios of 1.3 ± 0.1 and 1.6 ± 0.2 from, respectively, N V and C IV doublets, thus implying that the MAX gas is *not* entirely optically thin in either line. Permitted UV lines of C III at $\lambda 1176$ and $\lambda 2297$ are seen strongly in our FOS spectra at maximum light, but were not previously confirmed in *IUE* observations of HZ Her/Her X-1. Howarth & Wilson (1983b) caution that the detection of these latter lines might be in mild conflict with earlier determinations of the physical conditions of the MAX gas.

The strongest predicted Bowen-pumped oxygen line, O III $\lambda 3133$, is prominent in our FOS spectra of the MAX gas and, combined with our measure of He II $\lambda 1640$, provides a high

S/N determination of the efficiency, R , with which helium photons are converted into oxygen photons via the fluorescence process. While earlier, but uncertain, *IUE* results had found an uncomfortably high value of $R \approx 2$, our FOS-determined value of $R = 0.6$ (assuming case B) is below the recombination limit of $R = 1$. The optical spectrum at maximum shows the blend—often also attributed to the Bowen mechanism—of C III/N III $\lambda\lambda 4640, 4650$ emission lines.

In the FOS UV spectra at mid-eclipse, the absence of the O III $\lambda 3133$ Bowen line is noteworthy. The optical spectrum at mid-eclipse also lacks the $\lambda\lambda 4640, 4650$ complex. This mutual disappearance lends support to the idea that the Bowen mechanism is indeed likely to also be responsible for the $\lambda\lambda 4640, 4650$ complex. That these Bowen-pumped lines are fully eclipsed also suggests that the Bowen emission line region is coincident with one of the traditionally suggested sites, i.e., the X-ray heated atmosphere of HZ Her, disk, etc. Aside from such emission, the FOS near-UV spectrum of Figure 2c and optical spectra of Figure 2d at minimum light are reasonable matches to those of a fairly normal late A or early F star (A8–F0).

However, the minimum light UV FOS spectrum of Figure 2a shows a rather surprising result. Despite the total eclipse (binary phase 0.000 ± 0.006) of the X-ray emitting neutron star (and the unobservability of the X-ray illuminated side of HZ Her), the spectrum shows strong UV emission from N V, Si IV + O IV], N IV], and C IV. The contemporaneous optical spectrum at mid-eclipse (Fig. 2d) also shows He II $\lambda 4686$ in emission. The physical conditions in this "MIN" gas that dominates the UV emission at mid-eclipse are obviously rather different than those in the MAX gas. For example, the lower density and temperature of the MIN gas are indicated by the greater relative strength of (the collisionally de-excitable) N IV] emission in the MIN gas, and the absence of O V emission. An initial comparison of the observed FOS spectrum of Figure 2a with simple model spectra suggests plausible MIN gas physical conditions of $15,000 \text{ K} \lesssim T \lesssim 33,000 \text{ K}$, $n_e \lesssim 10^{11} \text{ cm}^{-3}$, $N_p \gtrsim 10^{19} \text{ cm}^{-2}$, and an ionization parameter of $10^0 \lesssim \xi \lesssim 10^1$ (cgs units).

Both the FOS (Fig. 2a) and optical spectra (Fig. 2d) at minimum light confirm the presence of another site of hot gas in the system, a site that is evidently distinct from that producing the Bowen-related emission lines. This additional site is either noncoincident and/or more extended than the traditionally discussed locales of the disk and X-ray illuminated side of the A star. For example, our geometrical model tests indicate that a simple cylindrical disk of the size usually inferred for Her X-1 system should be fully occulted during the mid-eclipse FOS observations. Other workers have also found direct evidence for extended hot gas in their observation of residual X-ray flux at mid-eclipse, but it seems likely there are multiple hot extended components present with a range of physical conditions. Although the hot gas whose emission dominates the FOS UV light at phase 0.00 might be associated with an accretion disk corona, it is more likely the source is somewhat less hot (but extended) gas above and around the disk, or perhaps circumstellar material such as a stellar wind.

The observations discussed here were made as part of the FOS GTO program. We are indebted to our coinvestigators on the FOS Investigation Definition Team, R. Angel, F. Bartko, E. Beaver, R. Bohlin, M. Burbidge, A. Davidsen, H. Ford, R. Harms, and G. Hartig, as well as the rest of the

FOS science team, who helped to make this work possible. We thank M. Scott, J. Deeter, and P. Boynton for useful discussions, and R. McCray and I. Howarth for helpful comments on the manuscript. We gratefully acknowledge K. Coughlin

and R. Marx for their assistance in classifying the HZ Her spectra. A preliminary report of this work has been given by Wachter et al. (1994). Financial support has been provided by NASA grant NAG5-1630.

REFERENCES

- Arons, J. 1973, *ApJ*, 184, 539
 Baum, S. 1994, *The HST Data Handbook* (Baltimore: STScI)
 Begelman, M. C., & McKee, C. F. 1983, *ApJ*, 271, 89
 Blair, W. P., et al. 1994, in preparation
 Bochkarev, N. G., & Karitskaya, E. A. 1989, *Ap&SS*, 154, 189
 Bohlin, R. C. 1975, *ApJ*, 200, 402
 Boyle, S. J., & Howarth, I. D. 1988, in *A Decade of UV Astronomy with the IUE Satellite*, Vol. 1., ed. E. J. Rolfe (Noordwijk: ESA), 133
 Boyle, S., Howarth, I., Wilson, R., & Raymond, J. 1986, in *New Insights in Astrophysics: 8 Years of UV Astronomy with IUE*, ed. E. J. Rolfe (Noordwijk: ESA), 471
 Boynton, P. E., Crosa, L. M., & Deeter, J. E. 1980, *ApJ*, 237, 169
 Choi, C. S., Dotani, T., Nagase, F., Makino, F., Deeter, J. E., & Min, K. W. 1994a, in preparation
 Choi, C. S., Nagase, F., Makino, F., Dotani, T., & Min, K. W. 1994b, *ApJ*, 422, 799
 Cordova, F. A., & Howarth, I. D. 1987, in *Exploring the Universe with the IUE Satellite*, ed. Y. Kondo et al. (Dordrecht: Reidel), 395
 Crampton, D., & Hutchings, J. B. 1974, *ApJ*, 191, 483
 Crosa, L. M., & Boynton, P. E. 1980, *ApJ*, 235, 999
 Davidsen, A., Henry, J. P., Middleditch, J., & Smith, H. E. 1972, *ApJ*, 177, L97
 Davidson, K., & Ostriker, J. P. 1973, *ApJ*, 179, 585
 Deeter, J. E. 1992, private communication
 Deeter, J. E., Boynton, P. E., Miyamoto, S., Kitamoto, S., Nagase, F., & Kawai, N. 1991, *ApJ*, 383, 324
 Dupree, A. K., et al. 1978, *Nature*, 275, 400
 Gerend, D., & Boynton, P. E. 1976, *ApJ*, 209, 562
 Giacconi, R., Gursky, H., Hellogg, E., Levinson, R., Schreier, E., & Tananbaum, H. 1973, *ApJ*, 184, 227
 Gursky, H., et al. 1980, *ApJ*, 237, 163
 Hatchett, S., Buff, J., & McCray, R. 1976, *ApJ*, 206, 847
 Heiles, C. 1975, *A&AS*, 20, 37
 Howarth, I. D., & Wilson, R. 1983a, *MNRAS*, 202, 347
 ———. 1983b, *MNRAS*, 204, 1091
 Jacoby, G. H., Hunter, D. A., & Christian, C. A. 1984, *ApJS*, 56, 257
 Joss, P. C., & Rappaport, S. A. 1984, *ARAA*, 22, 537
 Kallman, T. R., & Krolik, J. H. 1993, *XSTAR User's Guide*
 Koo, D. C., & Kron, R. G. 1977, *PASP*, 89, 285
 Kriss, G. A. 1994, in *Proc. of the Third Conference on Astrophysics Data Analysis and Software Systems*, ed. D. Crabtree (San Francisco: ASP), in press
 Kriss, G. A., Blair, W. P., & Davidsen, A. F. 1992, *FOS Calibration Rep. No. 70*, STScI
 Liu, X. W., & Danziger, J. 1993, *MNRAS*, 261, 465
 Margon, B., & Cohen, J. G. 1978, *ApJ*, 222, L33
 Mason, K. O., Murdin, P. G., Tuohy, I. R., Seitzer, P., & Branduardi-Raymont, G. 1982, *MNRAS*, 200, 793
 Mavromatakis, F. 1993, *A&A*, 273, 147
 McClintock, J. E., Canizares, C. R., & Tarter, C. B. 1975, *ApJ*, 198, 641
 McCray, R., & Hatchett, S. 1975, *ApJ*, 199, 196
 McCray, R. A., Shull, J. M., Boynton, P. E., Deeter, J. E., Holt, S. S., & White, N. E. 1982, *ApJ*, 262, 301
 Mihara, T., Ohashi, T., Makishima, K., Nagase, F., Kitamoto, S., & Koyama, K. 1991, *PASJ*, 43, 501
 Oke, J. B. 1976, *ApJ*, 209, 547
 Parmar, A. N., Pietsch, W., McKechnie, S., White, N. E., Trümper, J., Voges, W., & Barr, P. 1985, *Nature*, 313, 119
 Priedhorsky, W. C., & Holt, S. S. 1987, *Space Sci. Rev.*, 45, 291
 Schachter, J., Filippenko, A. V., & Kahn, S. M. 1989, *ApJ*, 340, 1049
 Tananbaum, H., Gursky, H., Kellog, E. M., Levinson, R., Schreier, E., & Giacconi, R. 1972, *ApJ*, 174, L143
 Voges, W., Kahabka, P., Ögelmen, H., Pietsch, W., & Trümper, J. 1985, *Space Sci. Rev.*, 40, 339
 Vrtilik, S. D., & Halpern, J. P. 1985, *ApJ*, 296, 606
 Wachter, S., Anderson, S. F., Margon, B., & Downes, R. A. 1994, in *Proc. of the 4th Annual Maryland Astrophysics Conference (AIP)*, in press
 White, N. E., Swank, J. H., & Holt, S. S. 1983, *ApJ*, 270, 711